

# 1 Modelling the vertical gradient of nitrogen dioxide in 2 an urban area

---

3 Marloes Eeftens<sup>1,2\*</sup>, Danyal Odabasi<sup>1,2</sup>, Benjamin Flückiger<sup>1,2</sup>, Mark Davey<sup>1,2</sup>, Alex Ineichen<sup>1,2</sup>, Christian  
4 Feigenwinter<sup>2</sup>, Ming-Yi Tsai<sup>1,2,3</sup>

## 5 **Affiliations:**

6 1. Swiss Tropical and Public Health Institute, Basel, Switzerland

7 2. University of Basel, Basel, Switzerland

8 3. Dept. of Environmental and Occupational Health Sciences, University of Washington, Seattle,

9 USA

## 10 **Corresponding author:**

11 Marloes Eeftens

12 E-mail: marloes.eeftens@swisstph.ch

13 Department of Epidemiology and Public Health

14 Swiss Tropical and Public Health Institute

15 Socinstrasse 57, P.O. Box 4002 Basel, Switzerland

16 Telephone: +41 61 284 87 25

17 Fax: +41 61 284 81 05

## 18 **Keywords:**

19 Air pollution, Vertical gradient, Land Use Regression, NO<sub>2</sub>, decay

## 20 **Sources of financial support:**

21 This work was supported by the Forschungsfonds University of Basel.

## 22 **Competing interest:**

23 The authors declare they have no competing financial interest.

24 **Abbreviations:**

25 LUR: Land use regression

26 LOOCV: Leave-one-out cross-validation

27 NO<sub>2</sub>: Nitrogen dioxide

28 RMSE: Root mean squared error

29 SVF: Sky view factor

30 **Acknowledgments:**

31 We thank all the study participants who provided a place to perform our measurements.

32 **Abstract**

33 Introduction

34 Land use regression models environmental predictors to estimate ground-floor air pollution  
35 concentration surfaces of a study area. While many cities are expanding vertically, such models  
36 typically ignore the vertical dimension.

37 Methods

38 We took integrated measurements of NO<sub>2</sub> at up to three different floors on the facades of 25  
39 buildings in the mid-sized European city of Basel, Switzerland. We quantified the decrease in NO<sub>2</sub>  
40 concentration with increasing height at each facade over two 14-day periods in different seasons.  
41 Using predictors of traffic load, population density and street configuration, we built conventional  
42 land use regression (LUR) models which predicted ground floor concentrations. We further evaluated  
43 which predictors best explained the vertical decay rate. Ultimately, we combined ground floor and  
44 decay models to explain the measured concentrations at all heights.

45 Results

46 We found a clear decrease in mean nitrogen dioxide concentrations between measurements at  
47 ground level and those at higher floors for both seasons. The median concentration decrease was  
48 8.1% at 10m above street level in winter and 10.4% in summer. The decrease with height was  
49 sharper at buildings where high concentrations were measured on the ground and in canyon-like  
50 street configurations. While the conventional ground floor model was able to explain ground floor  
51 concentrations with a model R<sup>2</sup> of 0.84 (RMSE 4.1 µg/m<sup>3</sup>), it predicted measured concentrations at all  
52 heights with an R<sup>2</sup> of 0.79 (RMSE 4.5 µg/m<sup>3</sup>), systematically overpredicting concentrations at higher  
53 floors. The LUR model considering vertical decay was able to predict ground floor and higher floor  
54 concentrations with a model R<sup>2</sup> of 0.84 (RMSE 3.8 µg/m<sup>3</sup>) and without systematic bias.

55 Discussion

56 Height above the ground is a relevant determinant of outdoor residential exposure, even in medium-  
57 sized European cities without much high-rise. It is likely that conventional LUR models overestimate  
58 exposure for residences at higher floors near major roads. This overestimation can be minimized by  
59 considering decay with height.

## 60 **Introduction**

61 In epidemiological studies done in large populations, exposure to air pollution is typically modelled.  
62 Land use regression (LUR) takes actual measurement data obtained from a limited number of  
63 monitors distributed throughout the study area and environmental information such as land use,  
64 proximity to roads, traffic intensity population density and other predictors, typically obtained from  
65 geographical information systems, aiming to predict detailed spatial contrasts (de Hoogh et al., 2016;  
66 de Hoogh et al., 2017; Eeftens et al., 2016; Hoek et al., 2008). Typical air pollution LUR models take  
67 into account horizontal proximity to a source, but study participants living in the same building but  
68 on different floors are attributed the same exposure estimate, which may not be accurate. It is  
69 possible that floor of residence is related to health, as suggested by a recent study which found that  
70 higher floors have lower mortality rates in Switzerland(Panczak et al., 2013).

71 Numerous studies have measured vertical gradients for individual streets as was recently reviewed  
72 by Sajani et al., (2018). Typically, studies found that in urban areas, levels of many pollutants  
73 decrease with increasing height, among them NO<sub>2</sub> (Lufthygieneamt beider Basel, 1993; Meng et al.,  
74 2008; Tsai and Chen, 2004; Zauli-Sajani et al., 2018), a marker for fossil fuel combustion by motorized  
75 traffic. The majority of these studies have focused on Asian cities which differ in pollutant sources,  
76 population density, and street setting (e.g., many high-rise buildings) and are therefore not directly  
77 comparable to moderate sized cities in Europe. Moreover, these studies typically measured the  
78 vertical gradient at a single or only at several buildings, allowing for the calculation of only one or  
79 several decay rates. To date, we only know of three other LUR studies which included height above  
80 the ground (floor level) as a model predictor, all are from Asia.(Barratt et al., 2018; Ho et al., 2015;  
81 Wu et al., 2014) In two Taiwanese studies, including floor level added substantially to the predictive  
82 power of a LUR model for PM<sub>2.5</sub> (mass of particulate matter with a diameter <2.5 micrometer), and  
83 several of its elemental constituents.(Ho et al., 2015; Wu et al., 2014) Another study from Hong Kong  
84 calculated vertical decay rates for black carbon and PM<sub>2.5</sub>, but due to a limited number of paired  
85 vertical sites, it was not possible to let the decay rate vary depending on local conditions.(Barratt et

86 al., 2018) Instead, decay rates were assumed to be the same across the entire region in the LUR  
87 model in the model application for epidemiological exposure estimation.(Barratt et al., 2018) This  
88 study aims to characterize vertical gradients in concentrations of NO<sub>2</sub> at many locations and  
89 investigate how these gradients may be related to geographical predictors and street configuration.  
90 We present and evaluate a three dimensional LUR model for NO<sub>2</sub> in which vertical decay is fully  
91 integrated.

## 92 **Methods**

### 93 **Study design**

94 We selected 25 buildings, adjacent to a diverse variety of streets in the canton of Basel Stadt,  
95 Switzerland, which had a population of 198'000 in 2016.(Statistisches Amt Basel Stadt, 2017) We  
96 aimed to represent the full range of traffic densities and street configurations, and over-represent  
97 busy and canyon-like streets, where we expected higher concentrations (Figure 1). Measurements  
98 took place simultaneously at all sites over a period of two weeks in the winter (25 February to 11  
99 March 2016) and were repeated in summer (13 June to 29 June 2016). Samplers were installed and  
100 collected over two consecutive days each round. On each building, we installed three integrated NO<sub>2</sub>  
101 passive samplers from the company PASSAM AG(Passam - Laboratory for environmental analysis and  
102 air pollution) in a vertical line by attaching the sampler tubes in shelters on the external wall or  
103 windows facing the street. Buildings differed in their facade structure, so having consistently the  
104 same spacing between ground floor and the higher samplers was not feasible. Instead, the lowest of  
105 the three measurements was always at the ground floor, between 1.8 and 2.9 meter above ground  
106 and the other two samplers were placed at floors 1 to 6, up to 20 meters above street level,  
107 attempting to maximize the vertical spread, but constrained by the residents' willingness to  
108 participate. The exact installation height of each sampler was determined using a Bosch PLR 50 Laser  
109 Measure. The height of the building to which the samplers were attached, the height of the building  
110 on the opposite side of the street and the street width were measured to calculate the canyon aspect

111 ratio: the average building height on both sides of the street ( $h_1$  and  $h_2$ ) divided by the street width  
112 ( $w$ ):  $(h_1+h_2)/(2*w)$ . During both summer and winter, off-peak (09:00-16:00) traffic density at each  
113 site was counted for 30 Minutes. To assess the quality of the measurements, we took a total of 8  
114 field blanks and 12 duplicates during the winter and summer seasons.

## 115 **Geographical predictor data**

116 A list of 66 spatial predictors were derived in different buffers, following previous land use regression  
117 studies in small geographic areas.(Cyrus et al., 2012; Eeftens et al., 2013; Eeftens et al., 2012; Eeftens  
118 et al., 2016) The following geographic information was available:

- 119 - Information on population density was available from the 100x100m grid the Federal  
120 Statistical Office published in 2011. The number of inhabitants was derived in six different  
121 buffers of 100, 250, 500, 750, 1000 and 5000m.
- 122 - Information on land cover was obtained from the Corine Land Cover 2006 Raster  
123 data.(European Environment Agency (EEA)) The original 44 classes were summarized into 7  
124 groups: airport, industry, natural, port, residential, water and urban green spaces, following  
125 earlier publications.(Beelen et al., 2009; Beelen et al., 2013; Eeftens et al., 2012) We derived  
126 the total area of each land use (in  $m^2$ ) in six different buffers of 100, 250, 500, 750, 1000 and  
127 5000m.
- 128 - A digital national road network (Vector 25) was available from SwissTopo. The SonBase Noise  
129 Database, available from the Federal Office for the Environment, provided modelled traffic  
130 intensity.(Swiss Bundesamt für Umwelt (BAFU), 2009) The length of each road segment in a  
131 buffer was multiplied by the traffic intensity on that segment, after which all segments were  
132 summed to obtain the traffic load for that buffer. Correlation between traffic load and locally  
133 conducted traffic counts validated this measure (Online Supplement 1). Road length (in m)  
134 and traffic load (in vehicles  $day^{-1}*m$ ) were calculated in eight different buffers of 25, 50, 75,  
135 100, 250, 500, 750, 1000m.

- 136 - The Institute of Meteorology, Climatology and Remote Sensing at the University of Basel  
137 provided a detailed 1x1m map of the sky view factor (SVF)(Lindberg and Grimmond, 2010), a  
138 unit-less measure for the canyon-like structure of urban streets, which was previously shown  
139 to improve air pollution models (Eeftens et al., 2013). The higher the sky view factor, the  
140 more of the sky is visible, and thus the higher the air exchange rate between the canyon and  
141 the air above. Correlations between aspect ratio (measured at each site) and SVF validated  
142 this measure (Online Supplement 1).
- 143 - Altitude information (in m above sea level) was available from the DHM25 of SwissTopo and  
144 was extracted for each point.(Bundesamt für Landestopographie, 2001)

145 Altitude, natural and urban green land use and sky view factor were assumed to have a negative  
146 effect on NO<sub>2</sub> concentration with increasing value and no a priori assumptions were made about the  
147 effect of water. All other predictors were assumed to have a positive effect on NO<sub>2</sub> concentration. No  
148 a priori assumptions were made on how these predictors affected the vertical decay.

### 149 **Land use regression modelling**

150 Following an earlier publication(Eeftens et al., 2016), the calculated predictors were screened prior  
151 to their evaluation in the LUR model. Predictors were discarded if fewer than five sites had a value  
152 different from the most frequently occurring value, if the maximum value was higher than  
153  $P90+3*(P90-P10)$  or the minimum value was lower than  $P10-3*(P90-P10)$ . All these criteria indicate  
154 an abnormal distribution and a model including such variables would likely yield unstable  
155 coefficients. We followed the same stepwise variable selection procedures as were used by several  
156 earlier studies.(Eeftens et al., 2012; Eeftens et al., 2016) Criteria for the inclusion of additional  
157 variables were: 1) an improvement in adjusted r-squared by at least 0.01; 2) ensuring the a priori  
158 defined direction of effect for all variables; 3) a p value smaller than 0.05; 4) a maximum Cook's D  
159 value of 1 for all sites; 5) a maximum Variance Inflation Factor (VIF) of 3 to minimize collinearity; 6)  
160 no change in the direction of previously included variables.

161 Firstly, NO<sub>2</sub> concentration at the ground floor was modelled for both summer and winter separately.  
162 We then combined both seasonal ground floor models into a mixed model by including an indicator  
163 for season and a random effect for site.

164 Vardoulakis et al. (2003) suggested that vertical profiles typically decrease exponentially with height.  
165 The concentration at any height can thus be determined by the ground concentration, the height and  
166 a decay constant  $k$  following Equation 1. Since we had multiple measurements per building, we fit an  
167 exponential model to determine  $k$  for each measurement site and for the winter and summer  
168 seasons. Deriving a second set of models, we then selected the predictors which best determined  $k$   
169 using the same variable selection method described above, adding a random effect for site. Seasonal  
170 models were combined into a model for both seasons, originally retaining all of the selected spatial  
171 predictors and the random intercept for site and adding an indicator for season. Any redundant  
172 spatial variables were excluded if the increased in AIC was less than 2, indicating that they did not  
173 substantially improve the combined model.

174 Equation 1:  $Concentration_{height} = Concentration_{ground} \times e^{k \times height}$ .

175 As a third step, the ground floor model and the model for  $k$  were combined by plugging the models  
176 for ground floor concentration and  $k$  into Equation 1, thereby extending the LUR to allow for the  
177 calculation of concentrations at any height and location in the city.

## 178 **Model diagnostics**

179 We derived model R<sup>2</sup> and RMSE, as well as cross-validation R<sup>2</sup> and RMSE for all models. We further  
180 validated all models by iteratively leaving each of the 25 buildings out entirely and predicting it using  
181 the remaining 24 buildings. For models M1 and M2, where we had a single observation per building,  
182 this was done using leave-one-out cross-validation (LOOCV), iteratively leaving out each one of 25  
183 sites and predicting its concentration based on the coefficients obtained from a model fit on the  
184 remaining 24 sites (Table 1). For the mixed models (M3-M9), this cross-validation was done by  
185 simultaneously leaving out all observations from that building from both seasons and using only the

186 fixed effects obtained from the remaining sites to predict up to six concentrations for that building  
187 (two seasons \* up to three different heights).

188 For the four models which were built using stepwise selection (M1, M2, M4 and M5), we assessed  
189 the chance that similarly high model  $R^2$  values could be obtained solely by chance, as suggested by  
190 Basagaña et al., 2012.(Basagaña et al., 2012) Using the dependent variables from the study ( $\text{NO}_2$  or  
191  $\text{k}$ ), we simulated the model building process 10,000 times using unique sets of randomly generated  
192 “predictor” variables, from a normal distribution with mean = 0 and standard deviation of 1. For each  
193 model, we then simulated the chance of finding a model based on random variables with an equally  
194 high or higher  $R^2$  than the model we selected.

## 195 **Used software**

196 All geographical predictor variables were derived in ArcGIS10. All statistical analyses were done in R  
197 version 3.3.2, using packages lme4 for the mixed models and ggplot for plotting.(R Core Team)

## 198 **Results**

### 199 **Measurements**

200 We found that  $\text{NO}_2$  concentrations were substantially higher in the winter season with a ground-floor  
201 median of  $35.1 \mu\text{g}/\text{m}^3$  (InterQuartile Range (IQR): 32.5-43.9) than in the summer season (median  
202  $23.2 \mu\text{g}/\text{m}^3$ , IQR: 20.2-34.8) (Figure 2). All field blanks indicated concentrations under or at the  
203 detection limit ( $\leq 0.4 \mu\text{g}/\text{m}^3$ ) indicating negligible contamination. Primary and duplicate samples were  
204 highly correlated ( $R^2$ : 0.94) and showed a low mean absolute difference of  $1.6 \mu\text{g}/\text{m}^3$ , indicating high  
205 reproducibility (Online Supplement 2).  $\text{NO}_2$  concentrations generally decreased with increasing  
206 height above the ground in both winter and summer. The decay constant  $k$  was calculated at a  
207 median of  $-0.0084 \text{ m}^{-1}$  in winter (IQR:  $-0.011 \text{ m}^{-1}$  to  $-0.00068 \text{ m}^{-1}$ ) and at a median of  $-0.011 \text{ m}^{-1}$  (IQR: -  
208  $0.017 \text{ m}^{-1}$  to  $-0.0015 \text{ m}^{-1}$ ) in summer. This translates to a median concentration reduction of 8.1% at  
209 10m above street level (IQR: 0.7% to 10.2%) in winter and 10.4% (IQR: 1.5% to 15.2%) in summer

210 (see Online Supplement 3). The decrease with height was sharper at buildings where higher NO<sub>2</sub>  
211 concentrations were measured at ground level: for an IQR increase in ground level NO<sub>2</sub>, *k* decreased  
212 by 0.011 m<sup>-1</sup> in winter and by 0.0078 m<sup>-1</sup> in summer. The spatial contrast in NO<sub>2</sub> was highest at the  
213 ground floor, and decreased with increasing height (Figure 2). The average temperature in winter  
214 was 4.0 °C with a relative humidity of 77%, in summer this was 17.8 °C and 75% relative humidity.

## 215 **LUR models**

216 Out of the 67 predictors derived for the study, 27 were dropped in the variable screening process,  
217 leaving 40 eligible for evaluation. The screening process mostly flagged variables with a limited  
218 number of <5 points with a different value than the most common; e.g. few sites were within 100,  
219 250 or 500m of an airport, port or industrial area and thus these variables were mostly 0. The on-site  
220 measurements of the aspect ratio and the SVF derived from GIS were highly correlated, as were the  
221 manual traffic counts and the GIS derived traffic load in 25m ( $R^2 = 0.60$  and  $R^2 = 0.81$  respectively,  
222 Online Supplement 1).

223 The ground floor models identified for the winter (M1) and summer (M2) included the same two  
224 predictor variables (traffic load in a 25m buffer and residential land use in a 5000m buffer) with very  
225 similar coefficients, and yielded similar  $R^2$ 's of 0.71 and 0.79, respectively (Table 1). The combined  
226 mixed model for both seasons (M3, with random effects for site) showed a large increase of 11.9  
227  $\mu\text{g}/\text{m}^3$  for season and again yielded similar coefficients to the season-specific models and a slightly  
228 higher  $R^2$  of 0.84. No interactions between season and GIS variables were significant. Ground floor  
229 models performed reasonably well in leave-one-out (M1 and M2) cross validation, yielding a 10-11%  
230 lower predictive power and slightly higher similar RMSE's of 4.9  $\mu\text{g}/\text{m}^3$  and 4.6  $\mu\text{g}/\text{m}^3$ . Leave-one-  
231 group-out (M3) cross validation on the mixed model (M3), yielded a similar RMSE of 4.5  $\mu\text{g}/\text{m}^3$  and  
232 only slightly lower predictive power, due to the relatively large but easy to predict difference in  
233 season.

234 The decay constant did not differ notably between the seasons: a median decay of  $-0.0084\text{m}^{-1}$  was  
235 calculated for winter and  $-0.011\text{m}^{-1}$  for summer (Figure 3). Typically,  $k$  was lower for sites surrounded  
236 by high traffic load and in streets with a low SVF. The winter model for the decay constant  $k$  (M4)  
237 explained a substantial part of the variability in  $k$  ( $R^2$  of 0.69), and included variables related to traffic  
238 load (25m) and road length (100m) in the close vicinity, residential land use (250m), as well as sky  
239 view factor (Table 1). The summer model (M5) did not perform as well ( $R^2$  of 0.37), but included the  
240 same traffic load (25m) predictor and sky view factor, which were selected for both models with very  
241 similar coefficients, indicating that the busier and the more canyon-like the street, the lower  $k$  was.  
242 When the season-specific models were combined (M6), season was evaluated as an additional  
243 predictor but was not included because it was not significant. Similarly, residential land use and road  
244 length were no longer significant in the model for both seasons, and were dropped. The combined-  
245 season model (M6) for  $k$  had a lower  $R^2$ , but performed similarly well in leave-one-group-out cross-  
246 validation.

247 For the models M7, M8 and M9,  $R^2$  was very similar to the ground level models ( $R^2$ 's of 0.67, 0.78,  
248 0.84, respectively). Leave-one-group-out cross-validation predictions were able to estimate the  
249 variability in measured concentrations well (Table 1).

250 For the four models which were built using stepwise selection (M1, M2, M4 and M5), we repeatedly  
251 simulated the chance of obtaining a model with at least the same  $R^2$  by evaluating 40 randomly  
252 generated predictor variables. For the ground floor models M1 and M2, only 2.3% and 0.1% of  
253 simulated models had  $R^2$  values equal to or higher than 0.71 and 0.79 respectively, none of which  
254 included as few as two predictors. This indicated that the chance of obtaining similarly good ground  
255 floor models by chance was very small. The winter model for  $k$  (M4) had an  $R^2$  of 0.69, and a similarly  
256 low chance of 2.6% (1.2% with 4 variables or fewer) of obtaining this result by chance. However, a  
257 model similar to the summer model for  $k$  (M5), which included 2 predictors and yielded an  $R^2$  of 0.37,  
258 was obtained by chance in 26% of simulations (12% with 2 predictors or fewer). This indicated that it  
259 was more likely that the M5 model was due to chance.

## 260 LUR predictions

261 Figure 4 shows the correlation between the measured NO<sub>2</sub> concentrations and the predictions as  
262 obtained from the models M3 (Figure 3A) and M9 (Figure 3B). Model predictions by the  
263 “conventional” ground floor LUR model (M3) differ by building but are otherwise the same,  
264 regardless of the height. In contrast, the predictions by model M9 show a clear effect of height within  
265 each building, and that the decay with height is site-dependent. Predictions from the model M9,  
266 which considers the height, agree better with the measured data, showing a correlation of 0.84 with  
267 the measured data (versus 0.79 for M3) and a lower RMSE of 3.78 µg/m<sup>3</sup> (versus 4.25 µg/m<sup>3</sup> for M3).  
268 Applying the winter and summer ground floor models (M1 and M2) to predict all 72 and 69 sites  
269 measured in the respective seasons, regardless of their height, yielded R<sup>2</sup>'s of 0.62 (RMSE 4.13  
270 µg/m<sup>3</sup>) for winter and 0.71 (RMSE 4.09 µg/m<sup>3</sup>) for summer. Both of the seasonal models considering  
271 height (M6 and M7) also explained more variability with R<sup>2</sup>'s of 0.67 (RMSE 3.86 µg/m<sup>3</sup>) for winter  
272 and 0.78 (3.63 µg/m<sup>3</sup>) for summer.

273 Figure 5 shows the prediction errors by both models M3 and M9 as a function of floor of residence.  
274 At the ground floor level, both models perform similarly well, but the ground floor model M3 is less  
275 able to accurately predict concentrations at higher floors, showing a significant overestimation for  
276 floors for the 3<sup>rd</sup>, 4<sup>th</sup> and higher floors. The model M9 which includes height as a predictor is able to  
277 derive unbiased concentration estimates for both the ground floor and all higher floors.

## 278 Discussion

279 We found a clear decrease in NO<sub>2</sub> concentration with increasing height in both winter and summer,  
280 which was more pronounced in streets with high ground-floor concentrations. We showed that  
281 conventional “ground floor” LUR models can be extended to include height, by introducing a decay  
282 constant, *k*, which—like the ground floor concentration—depends on locally important  
283 environmental characteristics, such as the street configuration (e.g., SVF) and the local traffic load.  
284 We showed that a ground floor LUR model for NO<sub>2</sub> developed in the conventional way over-

285 predicted concentrations at higher floors, whereas our LUR model considering concentration decay  
286 with height was able to predict ground floor and higher floor concentrations with similar accuracy.

## 287 **Determinants of vertical decay**

288 The study confirms earlier suggestions from a review by Hoek et al (2008) that LUR models give  
289 biased estimates at higher floors for buildings near major roads, where concentration decrease  
290 sharply with height, and that vertical gradients at urban background locations are limited.(Hoek et  
291 al., 2008) In addition, this study suggests that the lower SVF (the more canyon-like the street), the  
292 sharper the decay with height. This is likely due to a lower air exchange rate between the air inside  
293 the canyon and the air above the building canopy, leading to substantial pollutant build-up at lower  
294 levels.(Vardoulakis et al., 2003) The median decay constants of  $-0.0084\text{m}^{-1}$  (winter) and  $-0.011\text{m}^{-1}$   
295 (summer) were similar to the  $-0.012\text{m}^{-1}$  applied for  $\text{NO}_2$  in Barrat et al. (2018), and those reported by  
296 Zauli-Sajani et al. (2018), estimated to be  $-0.022\text{m}^{-1}$  in winter and  $-0.007\text{m}^{-1}$  in summer<sup>1</sup>. While all  
297 three previous LUR studies which considered height hypothesized that the decay rate may depend on  
298 street configuration, they were unable to derive any patterns.(Barratt et al., 2018; Ho et al., 2015;  
299 Wu et al., 2014) In 1993, a study by the Lufthygieneamt beider Basel (Air hygiene office of Basel) also  
300 reported a decay with height in a canyon-like street.(Lufthygieneamt beider Basel, 1993) An inverted  
301 vertical gradient was observed for the heating season in that study, because of the chimneys  
302 emitting  $\text{NO}_2$  at rooftop level.(Lufthygieneamt beider Basel, 1993) We indeed found that  $k$  was  
303 slightly higher (closer to  $0\text{m}^{-1}$ ) in winter across the whole city, but this was not statistically  
304 significant. Although this may suggests that vertical decay is indeed slightly reduced in the  
305 wintertime because of additional  $\text{NO}_2$  emissions at rooftop level, we did not see a flattening or  
306 inversion of the vertical gradient in the winter time as reported in the study from 1993. This could be  
307 due to more homes switching to district heating and/or cleaner alternative fuels since 1993 making  
308 ground floor emissions from traffic relatively important determinants of vertical decay.

---

<sup>1</sup> These numbers were not directly reported by Zauli-Sajani et al. (2018), but derived using Equation 1 from the heights (ground  $\sim 1.5\text{m}$ ,  $15\text{m}$ ,  $26\text{m}$ ,  $44\text{m}$ ,  $65\text{m}$ ), the winter  $\text{NO}_2$  concentrations ( $70.5\text{ }\mu\text{g}/\text{m}^3$ ,  $63.6\text{ }\mu\text{g}/\text{m}^3$ ,  $62.9\text{ }\mu\text{g}/\text{m}^3$ ,  $38.7\text{ }\mu\text{g}/\text{m}^3$ ,  $18.1\text{ }\mu\text{g}/\text{m}^3$ ) and the  $\text{NO}_2$  summer concentrations ( $41.2\text{ }\mu\text{g}/\text{m}^3$ ,  $34.4\text{ }\mu\text{g}/\text{m}^3$ ,  $32.1\text{ }\mu\text{g}/\text{m}^3$ ,  $30.0\text{ }\mu\text{g}/\text{m}^3$ ,  $25.3\text{ }\mu\text{g}/\text{m}^3$ ).

## 309 **Implications for exposure science**

310 Vertical gradients and street configuration are typically thought to be relevant mostly to high-density  
311 high-rise cities.(Barratt et al., 2018; Ho et al., 2015; Wu et al., 2014) Our measurements show that  
312 the concentration drop in NO<sub>2</sub> is also relevant for medium-sized European cities, and that considering  
313 decay with height can also improve LUR models commonly applied to assess residential air pollution  
314 exposure in epidemiological studies. Similar vertical gradients may exist in other cities, but this  
315 depends on whether (as in Basel) most local air pollutants are emitted by traffic at street level, rather  
316 than e.g. by industry or home heating installations, which typically emit at rooftop level. In addition,  
317 vertical gradients may depend on weather patterns and local topography. This is one of the first  
318 studies looking at vertical gradients; therefore, we advise caution in translating these findings into  
319 local policies, or assuming impacts on indoor and personal air pollution exposure.

## 320 **Strengths and limitations**

321 In this study, we only measured NO<sub>2</sub>, which is a good marker for traffic-related air pollutants. It is  
322 likely that other air pollutants which decay more slowly with increasing horizontal distance, such as  
323 particulate matter smaller than 2.5 or 10 µm (PM<sub>2.5</sub> or PM<sub>10</sub>), may also exhibit a less pronounced  
324 vertical gradient (Karner et al., 2010). In contrast, pollutants which decrease more rapidly than NO<sub>2</sub> in  
325 the horizontal plane, such as CO, NO and ultrafine particles, may do so in the vertical dimension as  
326 well due to their chemical transformation and coagulation properties.(Karner et al., 2010)

327 As we used two-week time-integrated measurements of NO<sub>2</sub> in two different seasons, we were  
328 unable to test how the ground floor concentrations and vertical gradients may depend on individual  
329 meteorological factors such as precipitation, relative humidity, sunshine hours, temperature, wind  
330 speed and wind direction. The two seasons captured substantial differences in many of these  
331 weather parameters (see Online Supplement 4). The ground floor concentrations clearly differed  
332 substantially between the winter and summer seasons, and hence season is an important predictor  
333 for ground floor concentration. However, the median and IQR of  $k$  only differed slightly by season,

334 and season was not ultimately a significant determinant. This indicates that in our study,  $k$  was likely  
335 not substantially influenced by weather.

336 Another limitation of the study is its limited sample size (25 buildings) in the horizontal plane, which  
337 was due to the limited scope and budget available for the study. Several earlier papers have raised  
338 concern about overfitting in LUR models based on small datasets.(Basagaña et al., 2012; Wang et al.,  
339 2012) We took care to restrict the number of variables using a screening and a priori set standards  
340 for the acceptance of variables into the model (see methods), reducing the chance that unrelated  
341 variables would be included merely by chance. In addition, we quantified the chance of obtaining  
342 models with similar explanatory power using 40 randomly generated predictors, showing that for the  
343 ground level models, this chance was very low. For the models for  $k$ , there was a higher chance, but  
344 considering that both seasonal models for  $k$  independently selected SVF and a small (25m) buffer  
345 traffic load estimate supports that these predictors are likely actually predictive of  $k$ .

346 Furthermore, it was challenging to recruit multiple apartments in a single building to take part in the  
347 study, and especially to find buildings on major roads with relatively high ground floor  
348 concentrations. Due to the limited number of three different heights per building, we only  
349 considered an exponential decay shape for the vertical gradient and did not consider shapes with a  
350 higher number of parameters.

## 351 **Conclusion**

352 Height above the ground is a relevant determinant of outdoor residential exposure to traffic related  
353 air pollutant NO<sub>2</sub>. The decrease with height is clearer in places with a high ground floor  
354 concentration. This study is one of the first studies to develop a land use regression model which  
355 incorporates height above the ground as a predictor variable. This model outperformed a  
356 conventional ground-floor LUR model fitted using only measurements at street level in predicting  
357 concentrations at higher floors. The conventional LUR model overestimated exposure at higher

358 floors, particularly for residences where relatively high NO<sub>2</sub> concentrations were measured at ground  
359 level near major roads. This overestimation may be minimized by considering decay with height.

## 360 **References**

- 361 Barratt B, Lee M, Wong P, Tang R, Tsui TH, Cheng W, et al. A Dynamic Three-Dimensional Air  
362 Pollution Exposure Model for Hong Kong. HEI Research Report number 194 2018.
- 363 Basagaña X, Rivera M, Aguilera I, Agis D, Bouso L, Elosua R, et al. Effect of the number of  
364 measurement sites on land use regression models in estimating local air pollution.  
365 Atmospheric Environment 2012; 54: 634-642.
- 366 Beelen R, Hoek G, Pebesma E, Vienneau D, de Hoogh K, Briggs DJ. Mapping of background air  
367 pollution at a fine spatial scale across the European Union. Science of The Total Environment  
368 2009; 407: 1852-1867.
- 369 Beelen R, Hoek G, Vienneau D, Eeftens M, Dimakopoulou K, Pedeli X, et al. Development of NO<sub>2</sub> and  
370 NO<sub>x</sub> land use regression models for estimating air pollution exposure in 36 study areas in  
371 Europe – The ESCAPE project. Atmospheric Environment 2013; 72: 10-23.
- 372 Bundesamt für Landestopographie. DHM25: Das digitale Höhenmodell der Schweiz. 2001.
- 373 Cyrus J, Eeftens M, Heinrich J, Ampe C, Armengaud A, Beelen R, et al. Variation of NO<sub>2</sub> and NO<sub>x</sub>  
374 concentrations between and within 36 European study areas: Results from the ESCAPE study.  
375 Atmospheric Environment 2012; 62: 374-390.
- 376 de Hoogh K, Gulliver J, van Donkelaar A, Martin RV, Marshall JD, Bechle MJ, et al. Development of  
377 West-European PM<sub>2.5</sub> and NO<sub>2</sub> land use regression models incorporating satellite-derived and  
378 chemical transport modelling data. Environmental Research 2016; 151: 1-10.
- 379 de Hoogh K, Héritier H, Stafoggia M, Künzli N, Kloog I. Modelling daily PM<sub>2.5</sub> concentrations at high  
380 spatio-temporal resolution across Switzerland. Environmental Pollution 2017.
- 381 Eeftens M, Beekhuizen J, Beelen R, Wang M, Vermeulen R, Brunekreef B, et al. Quantifying urban  
382 street configuration for improvements in air pollution models. Atmospheric Environment  
383 2013; 72: 1-9.
- 384 Eeftens M, Beelen R, de Hoogh K, Bellander T, Cesaroni G, Cirach M, et al. Development of Land Use  
385 Regression models for PM<sub>2.5</sub>, PM<sub>2.5</sub> absorbance, PM<sub>10</sub> and PM<sub>coarse</sub> in 20 European study  
386 areas; results of the ESCAPE project. Environmental Science & Technology 2012; 46: 11195-  
387 205.
- 388 Eeftens M, Meier R, Schindler C, Aguilera I, Phuleria H, Ineichen A, et al. Development of land use  
389 regression models for nitrogen dioxide, ultrafine particles, lung deposited surface area, and  
390 four other markers of particulate matter pollution in the Swiss SAPALDIA regions.  
391 Environmental Health 2016; 15: 53.
- 392 European Environment Agency (EEA). Implementation and achievements of CLC2006. Available from:  
393 <https://www.eea.europa.eu/data-and-maps/data/clc-2006-raster-4> [Last accessed 21 August  
394 2018].

- 395 Ho C-C, Chan C-C, Cho C-W, Lin H-I, Lee J-H, Wu C-F. Land use regression modeling with vertical  
396 distribution measurements for fine particulate matter and elements in an urban area.  
397 Atmospheric Environment 2015; 104: 256-263.
- 398 Hoek G, Beelen R, de Hoogh K, Vienneau D, Gulliver J, Fischer P, et al. A review of land-use regression  
399 models to assess spatial variation of outdoor air pollution. Atmospheric Environment 2008;  
400 42: 7561-7578.
- 401 Karner AA, Eisinger DS, Niemeier DA. Near-Roadway Air Quality: Synthesizing the Findings from Real-  
402 World Data. Environmental Science & Technology 2010; 44: 5334-5344.
- 403 Lindberg F, Grimmond C. Continuous sky view factor maps from high resolution urban digital  
404 elevation models. Climate Research 2010; 42: 177-183.
- 405 Lufthygieneamt beider Basel. Höhenabhängigkeit der NO<sub>2</sub>-Belastung (in German). Study report 1993.
- 406 Meng ZY, Ding GA, Xu XB, Xu XD, Yu HQ, Wang SF. Vertical distributions of SO<sub>2</sub> and NO<sub>2</sub> in the lower  
407 atmosphere in Beijing urban areas, China. Science of The Total Environment 2008; 390: 456-  
408 465.
- 409 Panczak R, Galobardes B, Spoerri A, Zwahlen M, Egger M. High life in the sky? Mortality by floor of  
410 residence in Switzerland. European Journal of Epidemiology 2013; 28: 453-462.
- 411 Passam - Laboratory for environmental analysis and air pollution. Company website. Available from:  
412 <http://www.passam.ch/wp/> [Last accessed 21 August 2018].
- 413 R Core Team. R: A language and environment for statistical computing. R Foundation for Statistical  
414 Computing, Vienna, Austria. Available from: <https://www.r-project.org/> [Last accessed 21  
415 August 2018].
- 416 Statistisches Amt Basel Stadt. Statistisches Jahrbuch des Kantons Basel-Stadt, Chapter 1: Bevölkerung  
417 (in German). 2017.
- 418 Swiss Bundesamt für Umwelt (BAFU). SonBase–The GIS Noise Database of Switzerland. Technical  
419 bases [English version] 2009.
- 420 Tsai MY, Chen KS. Measurements and three-dimensional modeling of air pollutant dispersion in an  
421 Urban Street Canyon. Atmospheric Environment 2004; 38: 5911-5924.
- 422 Vardoulakis S, Fisher BE, Pericleous K, Gonzalez-Flesca N. Modelling air quality in street canyons: a  
423 review. Atmospheric Environment 2003; 37: 155-182.
- 424 Wang M, Beelen R, Eeftens M, Meliefste K, Hoek G, Brunekreef B. Systematic evaluation of land use  
425 regression models for NO<sub>2</sub>. Environmental Science & Technology 2012; 46: 4481-9.
- 426 Wu C-F, Lin H-I, Ho C-C, Yang T-H, Chen C-C, Chan C-C. Modeling horizontal and vertical variation in  
427 intraurban exposure to PM<sub>2.5</sub> concentrations and compositions. Environmental Research  
428 2014; 133: 96-102.
- 429 Zauli-Sajani S, Marchesi S, Trentini A, Bacco D, Zigola C, Rovelli S, et al. Vertical variation of PM<sub>2.5</sub>  
430 mass and chemical composition, particle size distribution, NO<sub>2</sub>, and BTEX at a high rise  
431 building. Environmental Pollution 2018; 235: 339-349.
- 432

433 **Table 1**

434 Table 1: Model results for ground-floor models, the decay constant  $k$  and the final LUR including  
 435 height, for winter and summer seasons separately and combined.

Dependent variable	Model	Season	N	Structure <sup>a</sup>	R <sup>2</sup> RMSE	R <sup>2</sup> LO(G)OCV RMSE <sup>c</sup>
Ground floor NO <sub>2</sub>	M1	Winter	25	NO <sub>2, winter</sub> = 37.5+ 6.32*traffic load (25m)+ 3.47*residential land use (5000m)	0.71 4.2	0.59 4.9
	M2	Summer	25	NO <sub>2, summer</sub> = 25.5+ 7.17*traffic load (25m)+ 3.36*residential land use (5000m)	0.79 3.7	0.68 4.6
	M3	Both seasons <sup>b</sup>	50	NO <sub>2, both seasons</sub> = 25.8+ 11.9*winter + 7.09*traffic load (25m)+ 3.34*residential land use (5000m)	0.84 4.1	0.79 4.5
$k$ (the decay constant)	M4	Winter	25	$k_{winter}$ = -0.00956+ -0.00988 * traffic load (25m) + -0.00512 * residential land use (250m) + 0.00448 * SVF <sup>d</sup> + -0.00345 * road length (100m)	0.69 0.0055	0.61 0.0066
	M5	Summer	25	$k_{summer}$ = -0.0125 + 0.00811 * SVF <sup>d</sup> + -0.00632 * traffic load (25m)	0.37 0.011	0.23 0.012
	M6	Both seasons <sup>b</sup>	50	$k_{both seasons}$ = -0.0112 + -0.00750 * traffic load (25m) + 0.00632 * SVF <sup>d</sup>	0.43 0.0067	0.33 0.010
Models including height	M7	Winter <sup>b</sup>	72	NO <sub>2</sub> = ground floor concentration <sub>winter</sub> * exp( $k_{winter}$ * height)	0.67 3.9	0.55 4.5
	M8	Summer <sup>b</sup>	69	NO <sub>2</sub> = ground floor concentration <sub>summer</sub> * exp( $k_{summer}$ * height)	0.78 3.6	0.68 4.4
	M9	Both seasons <sup>b</sup>	141	NO <sub>2</sub> = ground floor concentration <sub>both seasons</sub> * exp( $k_{both seasons}$ * height)	0.84 3.8	0.79 4.0

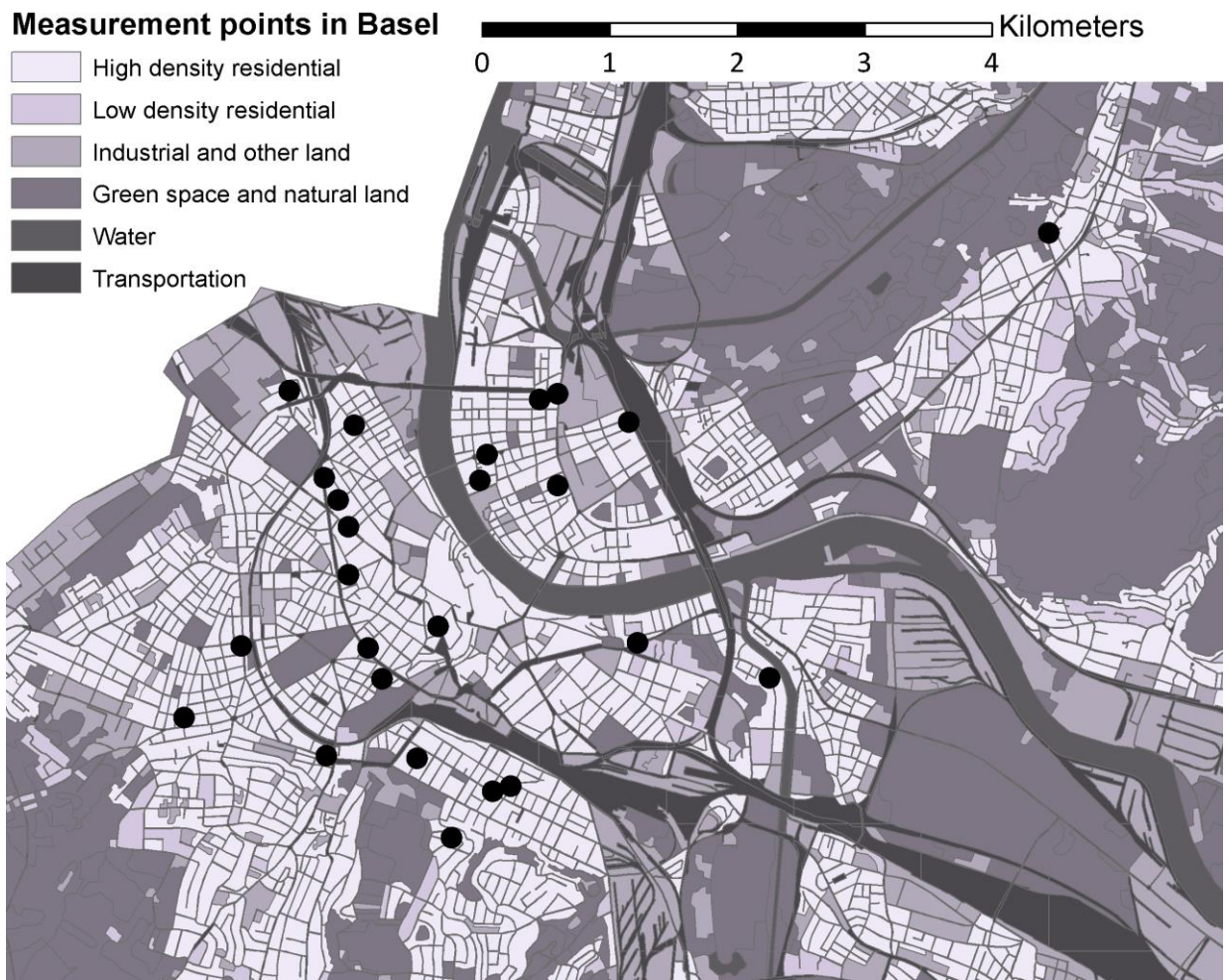
436 <sup>a</sup> Effects are shown for standardized variables, so the relative effect sizes of the predictors can be  
 437 compared.

438 <sup>b</sup> Mixed effects model with random intercept for site, reported model diagnostics are shown for fixed  
 439 effects only.

440 <sup>c</sup> LO(G)OCV = Leave One (Group) Out Cross Validation: all observations from one building (all heights,  
 441 all seasons) were left out simultaneously, which meant a single one for M1, M2, M4 and M5, two for  
 442 M3 and M6, up to three for M7 and M8, and up to six for M9. Concentrations were estimated using  
 443 only observations from other buildings.

444 <sup>d</sup> Sky view factor, see the method section; geographical predictor data.

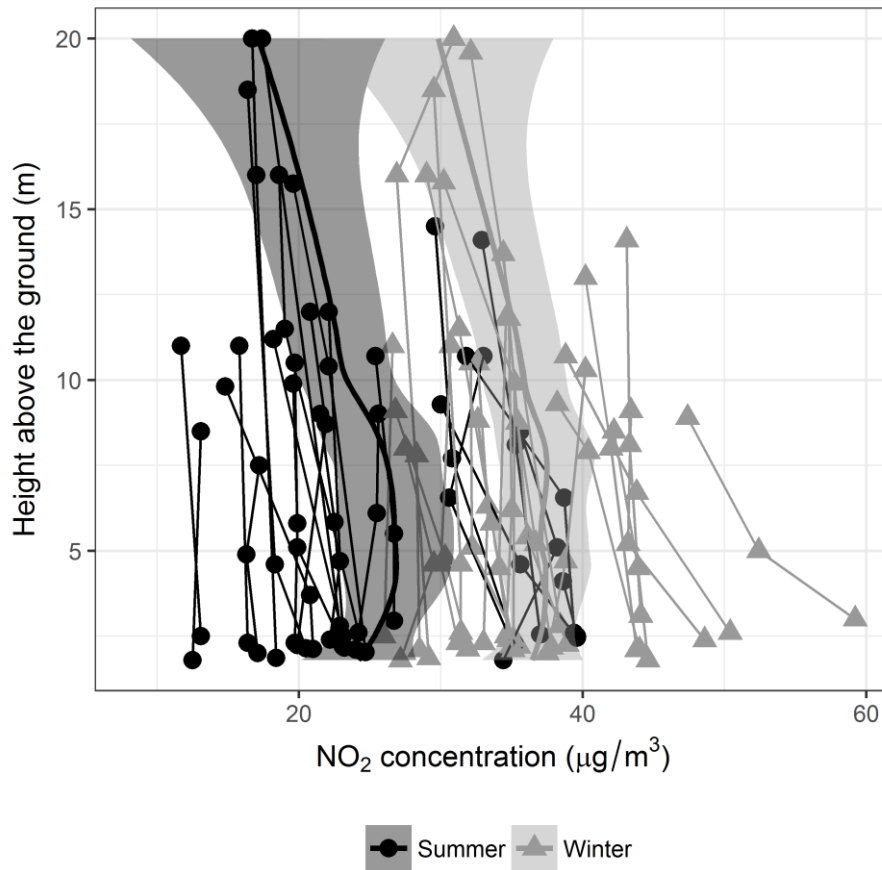
445 Figure 1: Map of measurement sites: black dots represent the 25 sampling sites in the canton of  
446 Basel Stadt, Switzerland.



447

448

449 Figure 2: NO<sub>2</sub> concentration by season: each line connects the concentrations measured at the  
450 different floors of the same building. The ribbons represent the general decreasing trend with  
451 increasing height above the ground, estimated by locally weighted regression (LOESS).



452

Figure 3: The decay constant  $k$  as calculated for all sites in the summer and winter period. Each point represents  $k$  as calculated for one of 25 sites measured in each season. The larger the point, the higher the traffic intensity around it: sites surrounded by more traffic generally have a lower  $k$  (i.e. a stronger decay). The darker the point, the more canyon-like the street, and thus the lower the SVF: sites in canyon-like streets generally have a lower  $k$  (i.e. a stronger decay). The diamond represents the mean, boxes the 25<sup>th</sup>, 50<sup>th</sup> and 75<sup>th</sup> percentiles, and whiskers extend to the smallest observation  $\geq$  the 25<sup>th</sup> percentile - 1.5 \* IQR (Interquartile Range) and the largest observation  $\leq$  the 75<sup>th</sup> percentile + 1.5 \* IQR. The Grey lines connect the same sites in different seasons.

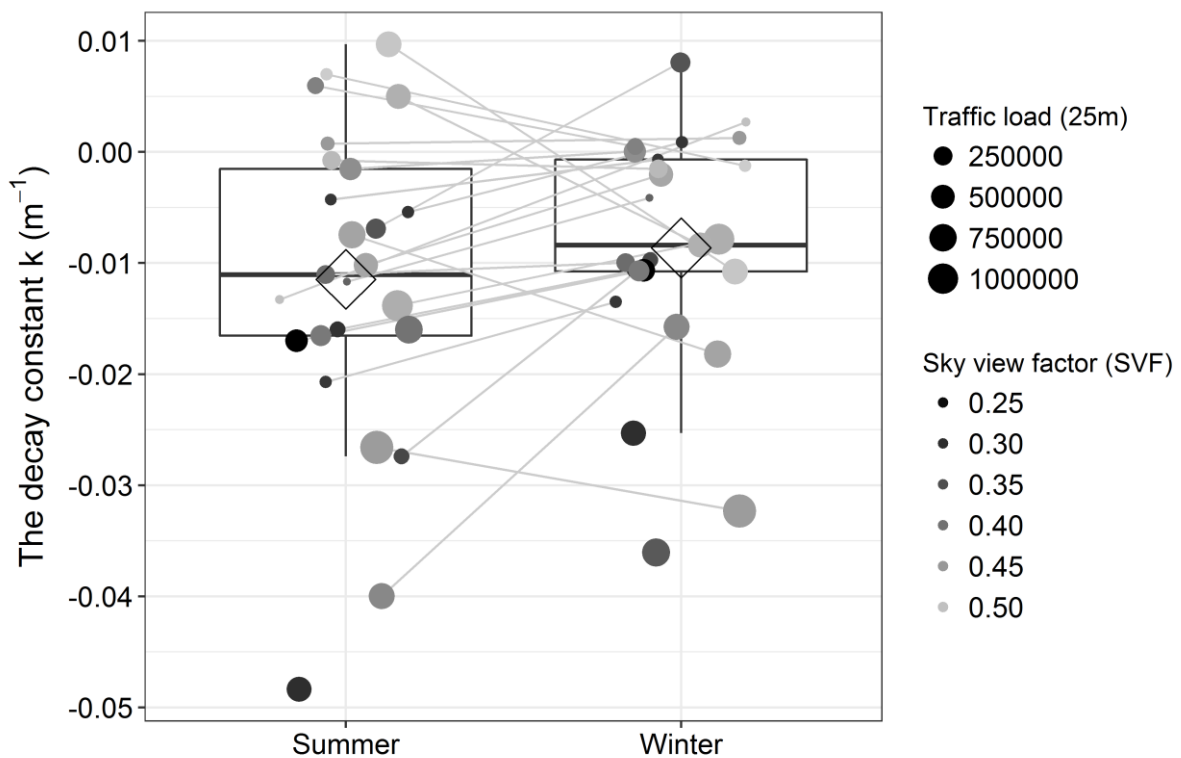


Figure 4: Model predictions for all 141 measurements by the ground floor model M3 (left) and by the model including height M9 (right). Connected points depict observations done in the same season at the same building. The ground floor model estimates the same concentration for the entire building facade, regardless of height, whereas the model including height shows a more realistic decay and predicts the observed decrease in NO<sub>2</sub> with height more accurately.

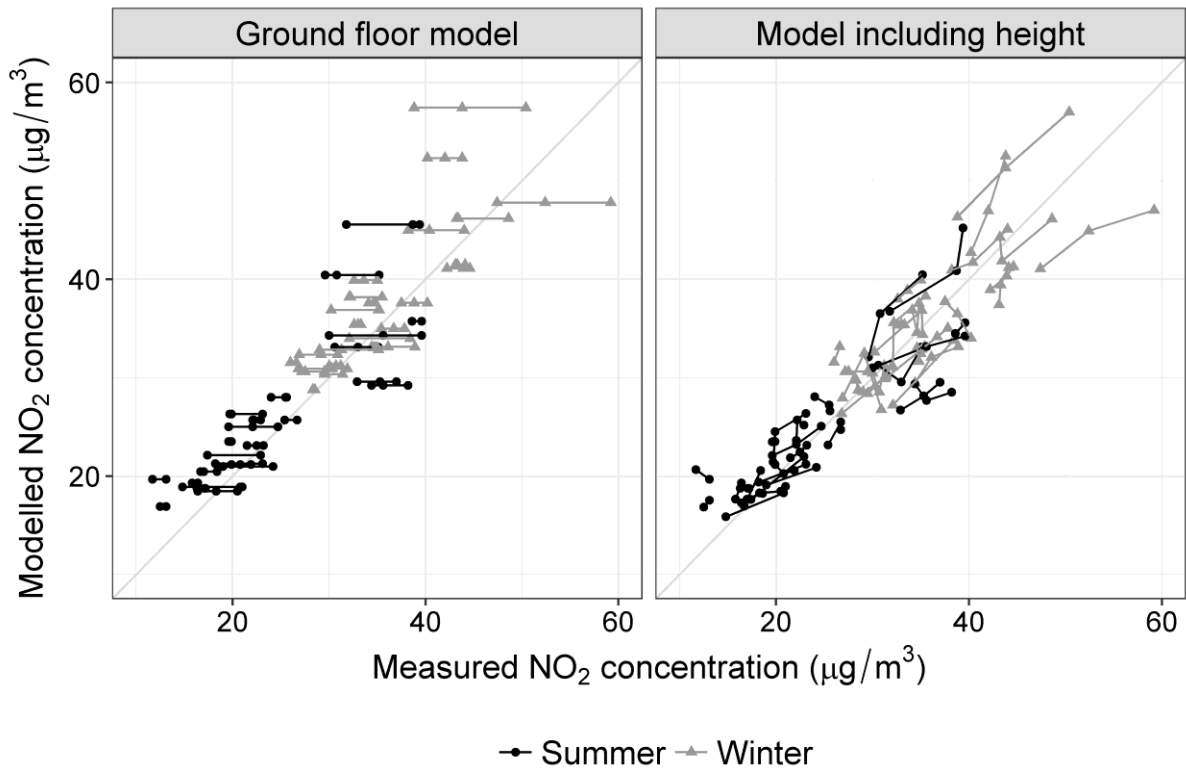


Figure 5: Model prediction error by floor for the model which did not include height and the model which considers decay with height. Note that the bias of the light grey model is increasingly positive for higher floors, indicating overestimation of the NO<sub>2</sub> concentration. The box shows the 25<sup>th</sup>, 50<sup>th</sup> and 75<sup>th</sup> percentiles, whiskers extend to the smallest observation  $\geq$  the 25<sup>th</sup> percentile - 1.5 \* IQR (Interquartile Range) and the largest observation  $\leq$  the 75<sup>th</sup> percentile + 1.5 \* IQR.

